

Supplementary Information (SI)

Optimisation of the Sorption of Selected Polycyclic Aromatic Hydrocarbons by Regenerable Graphene Wool

Adedapo O. Adeola ^a and Patricia B.C. Forbes ^{a*}

^a*Department of Chemistry, Faculty of Natural and Agricultural Sciences, University of Pretoria, Lynnwood Road, Hatfield, Pretoria 0002, South Africa.*

GC-MS ANALYSIS

PAH analysis was carried out with the aid of a gas chromatograph (GC, Agilent 6890) hyphenated with a mass spectrometer (MSD, Agilent 5975C) in electron impact ionization mode. The analytes (1 μL splitless injection) were separated on a Restek Rxi-PAH column with the following dimensions: 60 m long, 0.25 mm internal diameter and 0.10 μm film thickness. Helium gas of purity > 99 % (Afrox, Gauteng) was used as carrier gas in constant flow mode of 1 mL min^{-1} . The inlet temperature was at 275 $^{\circ}\text{C}$ and the GC oven temperature was held at 80 $^{\circ}\text{C}$ for 1 min, then ramped at 30 $^{\circ}\text{C min}^{-1}$ to 180 $^{\circ}\text{C}$, the subsequently to 320 $^{\circ}\text{C}$ at 5 $^{\circ}\text{C min}^{-1}$. The run-time for each injection was 35 min. The ionization potential was 70 eV, the source temperature was 230 $^{\circ}\text{C}$ and the quadrupole was at 150 $^{\circ}\text{C}$. A mass range of m/z 40-350 was recorded in full scan mode. For better sensitivity, the selective ion monitoring mode was employed to detect and quantify the analytes (Munyeza *et al.* 2018). Pure individual standards of pyrene and phenanthrene which had been dissolved in hexane were injected to determine the retention times and mass spectra thereof. Quantification of the selected PAHs was carried out using a six-point calibration with concentrations ranging from 16 to 1600 $\mu\text{g/L}$ for PHEN and 19 to 1800 $\mu\text{g/L}$ for PYR. The

calibration was derived from the plot of the target analyte peak area versus the concentration of the analyte.

ISOTHERM AND KINETIC DATA ANALYSIS

1. Adsorption Isotherm

Four different isotherm models were used to fit the adsorption experimental data. These models included the Freundlich, Langmuir, Temkin and Dubinin-Radushkevish isotherm models.

Freundlich Isotherm Model

The Freundlich model (FM), which is used commonly for quantifying hydrophobic organic compounds sorption equilibria has the following form;

$$\text{Nonlinear form: } q_e = K_f C_e^N \quad (3)$$

where q_e is the solid-phase concentration (ng/g) and C_e is the liquid-phase equilibrium concentration (mg/L). K_f is the sorption capacity-related parameter and N is the isotherm nonlinearity index, an indicator of site energy heterogeneity determined by linear regression of log-transformed data as shown below;

$$\text{Linear form: } \text{Log } q_e = \text{Log } K_f + \frac{1}{n} \text{Log } C_e \quad (4)$$

The Freundlich isotherm constants K_f and $1/n$ are evaluated from the intercept and the slope respectively, of the linear plot of $\log q_e$ versus $\log C_e$ (Rahman & Islam 2009).

Langmuir Isotherm Model

The Langmuir model (LM) describing site-limiting sorption equilibrium has the following form

$$\text{Langmuir: } q_e = \frac{q_m K_L C_e}{1 + K_L C_e} \quad (5)$$

where q_{\max} is the maximal sorption capacity and K_L is a solute–surface interaction energy-related parameter. The Langmuir equation can be rearranged to a linear form for the convenience of plotting and determination of the Langmuir constant (K_L). The values of q_m and K_L can be determined from the linear plot of $1/q_e$ versus $1/C_e$:

$$\text{Linear form: } \frac{1}{q_e} = \frac{1}{K_L q_{\max} C_e} + \frac{1}{q_{\max}} \quad (6)$$

The essential characteristics of the Langmuir isotherm parameters can be used to predict the affinity between the sorbate and the sorbent using the separation factor or dimensionless equilibrium parameter ' R_L ', expressed as in the following equation:

$$R_L = \frac{1}{1 + K_L C_0} \quad (7)$$

Where: K_L is the Langmuir constant and C_0 is the initial concentration of the PAHs. The value of the separation factor R_L provides important information about the nature of adsorption. The value of R_L is between 0 and 1 for favourable adsorption, while $R_L > 1$ represents unfavourable adsorption and $R_L = 1$ represents linear adsorption. The adsorption process is irreversible if $R_L = 0$ (Huang *et al.* 2003; Rahman & Islam 2009).

Dubinin-Radushkevish Isotherm Model

The Dubinin-Radushkevish (D-R) model was also used to fit experimental adsorption data using equation below;

$$\text{Nonlinear Form: } q_e = Q_D \exp(-k_{ad} \cdot \epsilon^2) \quad (8)$$

$$\text{Linear form: } \ln q_e = \ln Q_D - 2B_D RT \ln(1 + 1/C_e) \quad (9)$$

Where: Q_D is the theoretical maximum capacity (mol g^{-1}), B_D is the D-R model constant ($\text{kJ mol}^{-1} \text{K}^{-1}$), T is the absolute temperature (K) and R is the gas constant (kJ mol^{-1}). The mean energy of sorption, E (kJ mol^{-1}) is calculated from the relation;

$$E = 1/\sqrt{2B_D} \quad (10)$$

Q_D and B_D can be estimated from the intercept and slope of the plot of $\ln(q_e)$ versus $\ln(1 + 1/C_e)$ (Igwe & Augustine 2007)

Temkin Isotherm Model

The nonlinear and linearized form is expressed by the following equation:

$$\text{Nonlinear: } q_e = \frac{RT}{b_T} \ln K_T \cdot C_e \quad (11)$$

$$\text{Linear form: } q_e = \frac{RT}{b_T} \ln K_T + \frac{RT}{b_T} \ln C_e \quad (12)$$

Where: K_T (L g^{-1}) is the Temkin isotherm constant, b_T (J mol^{-1}) is a constant related to the heat of sorption and R ($8.314 \text{ J mol}^{-1} \text{K}^{-1}$) is the gas constant. A plot of q_e versus $\ln(C_e)$ gives a straight line equation from which K_T and b_T can be evaluated from the slope and the intercept (Mahamadi & Nharingo 2010).

Sips Isotherm Model

The Sips isotherm is used to describe localized adsorption without adsorbate-adsorbate interactions. Sips model can effectively reduce to Freundlich model or Langmuir model depending on the value of the equilibrium concentration (C_e). The Sips equation is given as;

$$\text{Nonlinear form: } q_e = \frac{K_s \cdot C_e^{\beta_s}}{1 + \alpha_s \cdot C_e^{\beta_s}} \quad (13)$$

$$\text{Linear form: } \frac{1}{q_e} = \frac{1}{Q_{\max} K_s} \left(\frac{1}{c_e} \right)^{1/n} + \frac{1}{Q_{\max}} \quad (14)$$

where K_s (1/mg) and Q_{\max} (mg/g) are the Sips equilibrium constant and maximum adsorption capacity values. The Sips isotherm equation includes the dimensionless heterogeneity factor, n , which describes the system's heterogeneity when its value is between 0 and 1. When, $n = 1$, the Sips equation implies homogeneous adsorption process (Langmuir) (Allen *et al.* 2004).

Adsorption Kinetics

Pseudo-First-Order Kinetic Model

It is given by equation below:

$$\text{Nonlinear form: } \frac{dq_t}{dt} = K_1 (q_e - q_t) \quad (15)$$

$$\text{Linear form: } \log(q_e - q_t) = \log q_e - \frac{k_1}{2.303} t \quad (16)$$

Where: q_t and q_e are the amount of solute sorbed per mass of sorbent (mg g^{-1}) at any time and at equilibrium, respectively, and k_1 is the rate constant of first-order sorption (min^{-1}). The straight-line plot of $\log(q_e - q_t)$ against t gives $\log(q_e)$ as slope and intercept equal to $k_1/2.303$. Hence the amount of solute sorbed per gram of sorbent at equilibrium (q_e) and the first-order sorption rate constant (k_1) can be evaluated from the slope and the intercept (Lagergren 1898; Kowanga *et al.* 2016)

Pseudo-Second-Order Kinetic Model

The model is represented as follows;

$$\text{Nonlinear form: } \frac{dq_t}{dt} = K_1 (q_e - q_t)^2 \quad (15)$$

$$\text{Linear Form: } \frac{t}{q_t} = \frac{1}{k_2 q_e^2} + \left(\frac{1}{q_e} \right) t \quad (16)$$

The kinetic parameters can be evaluated with straight-line plot of t/q_t against t , q_e and k_2 can be deduced from slope and intercept respectively. The initial sorption rate is defined by the following equation:

$$h = k_2 q_e^2 \quad (17)$$

Where: k_2 is the rate constant, q_t is the PAHs uptake capacity at any time t (Kalavathy et al. 2005).

FIGURES AND TABLES

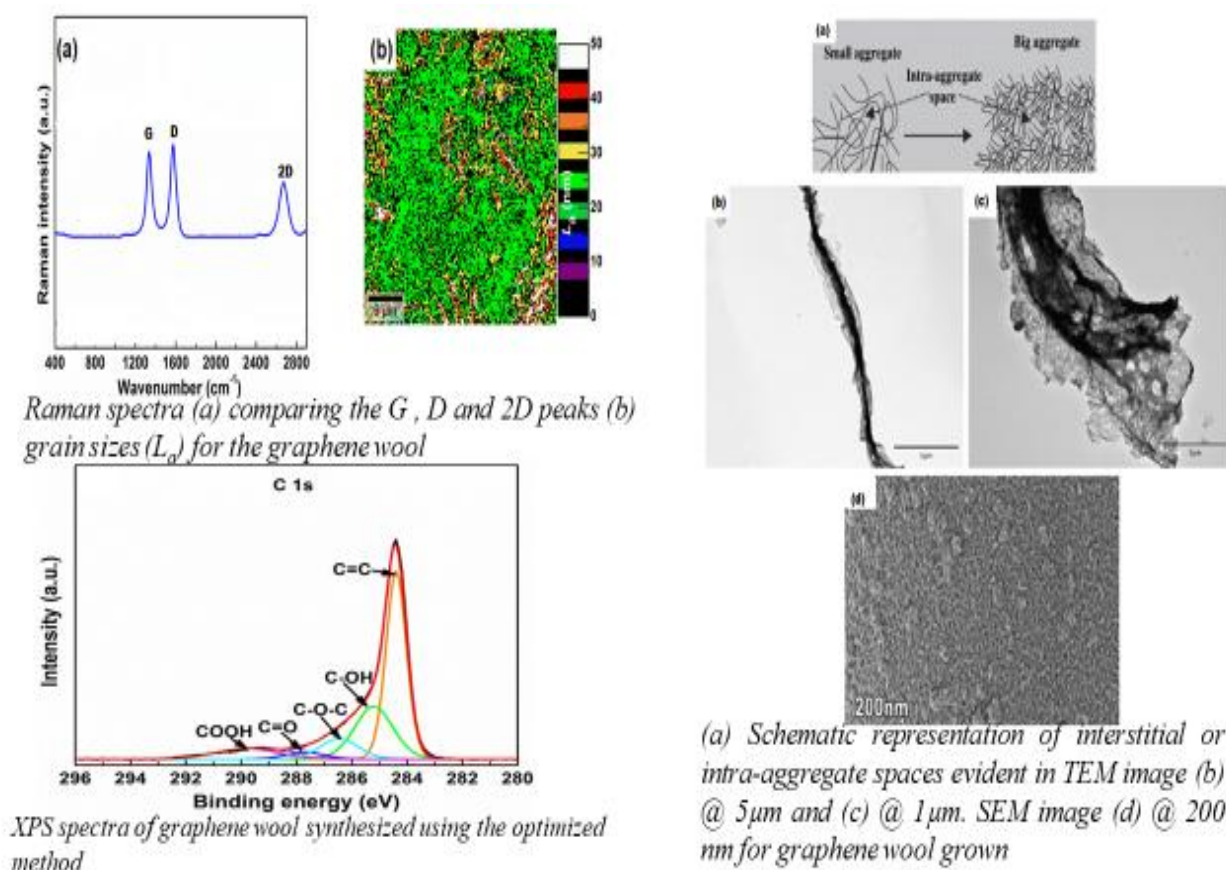


Figure S1: Raman spectroscopy (top-left), X-ray photoelectron spectroscopy (bottom-left), scanning electron microscopy and transmission electron microscopy analysis of graphene wool (right). Adapted from Schoonraad et al. (2020) with slight modifications.

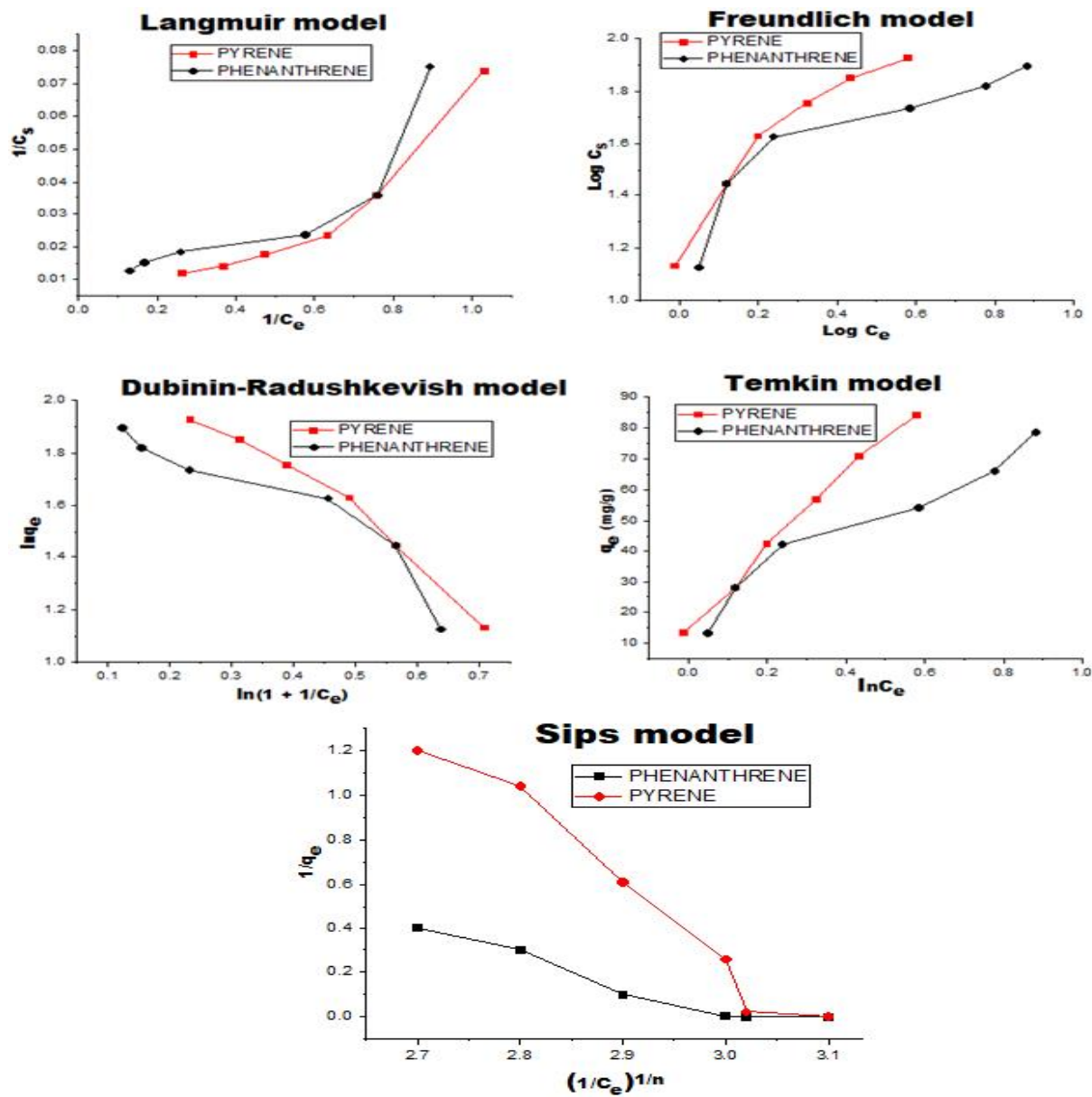


Figure S2: Adsorption isotherm models for phenanthrene and pyrene onto graphene wool in part-per-trillion concentrations (300-800 ng/L) (Experimental conditions: Dosage = 20 mg per 30 mL; mixing rate = 220 rpm; $T = 25 \pm 1$ °C; contact time = 24 hours; pH (PYR) = 6.7 ± 0.2 and pH (PHEN) = 6.8 ± 0.2).

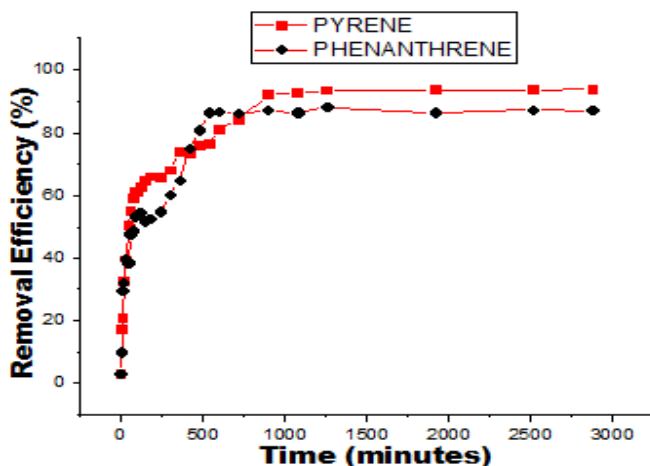


Figure S3: Profile of time-concentration pyrene and phenanthrene adsorption onto graphene wool (Experimental conditions: $C_o = 50 \text{ ng L}^{-1}$; dosage = 50 mg per 100 mL, mixing rate = 200 rpm, $T = 25 \pm 1 \text{ }^\circ\text{C}$; $\text{pH (PYR)} = 6.7 \pm 0.2$ and $\text{pH (PHEN)} = 6.8 \pm 0.2$).

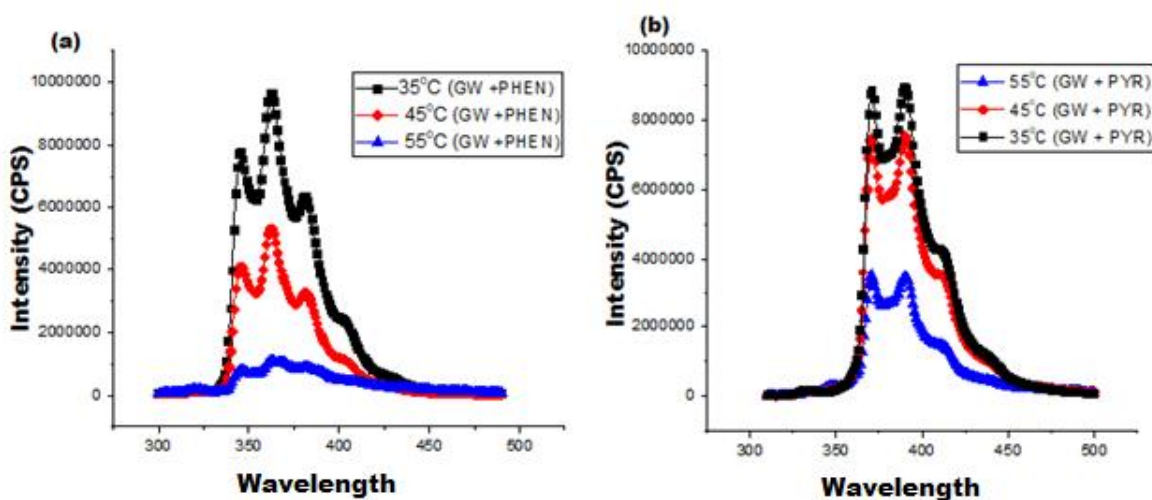


Figure S4: Fluorescence spectra of (a) Phenanthrene excited at 290 nm (b) Pyrene excited at 300nm; after interaction with GW at different temperatures. (Experimental conditions: mass of GW: 0.02 g; initial conc. of PAHs: 1 ppm, equilibration time: 24 h).

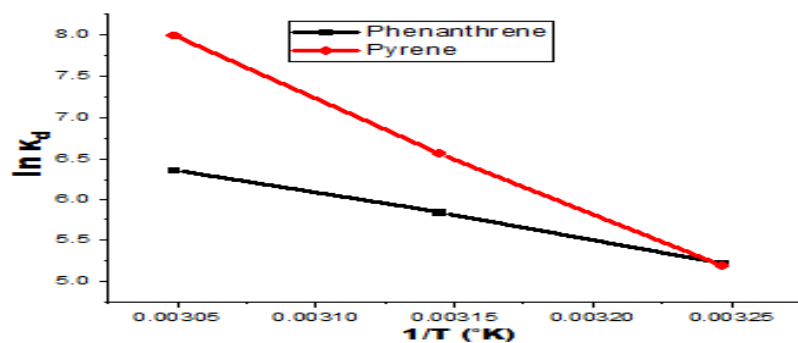
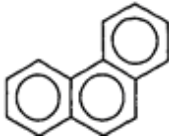



Figure S5: Van't Hoff equation for phenanthrene (PHEN) and pyrene (PYR) adsorption onto GW from solution.

Table S1: Selected physicochemical properties of the sorbates

PAH	Molecular structure	Molecular formula	^a LogK _{ow}	^a S _w	^a M _w	^b B _p	^c M _D (Å × Å × Å)
Phenanthrene (PHEN)		C ₁₄ H ₁₀	4.46	1.18	178.2	340	11.7 × 8.0 × 3.9
Pyrene (PYR)		C ₁₆ H ₁₀	5.13	0.135	202.3	404	11.7 × 9.3 × 3.9

Log K_{ow}: octanol–water partition coefficient, S_w: water solubility (mg L⁻¹), M_w: molecular weight (g cmol⁻¹), B_p: boiling points (°C). M_D: molecular dimension. Cited from ^a(Sun *et al.* 2013), ^b(Yakout & Daifullah 2013), (Potin *et al.* 2004)

Table S1: Coefficients of four different sorption isotherm models for phenanthrene and pyrene adsorption by graphene wool (GW) and their correlation coefficients (R^2) in part-per-trillion PAH concentrations (Experimental conditions: Dosage = 20 mg per 30 mL; mixing rate = 20 rpm; $T = 25 \pm 1$ °C; initial conc.: 300 - 800 ng L⁻¹; contact time = 24 hours; pH = 6.8 \pm 0.2 for PHEN and 6.9 + 0.2 for PYR).

Adsorption Isotherm Model	Parameter	PAH	
		Phenanthrene	Pyrenes
Dubinin-Radushkevish	Q_D (mol g ⁻¹)	4.62	4.02
	B_D (Kj mol ⁻¹ K ⁻¹)	1.47×10^{-4}	1.16×10^{-4}
	E (Kj mol ⁻¹)	58.14	65.36
	R^2	0.8770	0.9684
Freundlich	n	1.3797	0.7699
	K_f (ng ^{1-1/n} L ^{1/n} g ⁻¹)	18.4178	19.5140
	R^2	0.8139	0.9086
Langmuir	q_{max} (ng g ⁻¹)	1000	59.88
	K_L	0.016	0.2128
	R_L	0.510	0.072
	R^2	0.7441	0.8895
Sips	q_{max} (ng g ⁻¹)	3.39	0.83
	K_s (L mg ⁻¹)	9.6×10^{-4}	8.9×10^{-4}
	N	0.22	0.33
	R^2	0.9285	0.9893
Temkin	b_T (Kj mol ⁻¹)	174.48	305.87
	K_T (L g ⁻¹)	1.12×10^{-7}	1.67×10^{-7}
	R^2	0.9443	0.9928

Table S3: Effect of ionic strength on phenanthrene and pyrene removal by GW from aqueous solution

Ionic Strength	Parameters	Phenanthrene	Pyrene
0.01 mol L ⁻¹ [NaCl]	<i>R</i> ²	0.9246	0.9043
	<i>K</i> _d	166.24	506.57
	% Removal	98.61	99.37
0.1 mol L ⁻¹ [NaCl]	<i>R</i> ²	0.9586	0.9985
	<i>K</i> _d	319.97	612.87
	% Removal	98.76	99.38
1 mol L ⁻¹ [NaCl]	<i>R</i> ²	0.9770	0.9979
	<i>K</i> _d	340.85	742.34
	% Removal	99.11	99.59

Table S4: Effect of temperature on phenanthrene and pyrene removal from aqueous solution.

Temperature (°C)	Parameters	Phenanthrene	Pyrene
35	<i>R</i> ²	0.8702	0.9885
	<i>K</i> _d	184.69	242.99
	% Removal	98.5	98.7
45	<i>R</i> ²	0.9780	0.8894
	<i>K</i> _d	342.24	763.06
	% Removal	99.3	99.4
55	<i>R</i> ²	0.9466	0.9769
	<i>K</i> _d	578.8	2169.7
	% Removal	99.7	99.5

References

- Allen S. J., Mckay G. and Porter J. F. (2004). Adsorption isotherm models for basic dye adsorption by peat in single and binary component systems. *Journal of Colloid and Interface Science* (2), 322–33
- Huang W. L., Peng P. A. and Yu Z. Q. (2003). Effects of organic matter heterogeneity on sorption and desorption of organic contaminants by soils and sediments. *Applied Geochemistry* 18, 995-72.
- Igwe J. C. and Augustine A. A. (2007). Equilibrium sorption isotherm studies of Cd(II), Pb(II) and Zn(II) ions detoxification from waste water using unmodified and EDTA-modified maize husk. *Electronic Journal of Chemistry* 10(4), 535-48.
- Kalavathy M. H., Karthikeyan T., Rajgopal S. and Miranda L. R. (2005). Kinetic and isotherm studies of Cu(II) adsorption onto H₃PO₄-activated rubber wood sawdust. *Journal of Colloid and Interface Science* 292(2), 354-62.
- Kowanga K. D., Gatebe E., Mauti G. O. and Mauti E. M. (2016). Kinetic, sorption isotherms, pseudo-first-order model and pseudo-second-order model studies of Cu(II) and Pb(II) using defatted Moringa oleifera seed powder. *Journal of Phytopharmacology* 5(2), 71-8.
- Lagergren S. (1898). About the theory of so-called adsorption of soluble substances. *Kungliga Svenska Vetenskapsakademiens Handlingar, Band 24*, 1-29.
- Mahamadi C. and Nharingo T. (2010). Utilization of water hyacinth weed (*Eichhornia crassipes*) for the removal of Pb(II), Cd(II) and Zn(II) from aquatic environments: an adsorption isotherm study. *Environmental Technology* 31(11), 1221-8.

- Munyeza C. F., Dikale O., Rohwer E. R. and Forbes P. B. C. (2018). Development and optimization of a plunger assisted solvent extraction method for polycyclic aromatic hydrocarbons sampled onto multi-channel silicone rubber traps. *Journal of Chromatography A* 1555, 20-9.
- Potin O., Veignie E. and Rafin C. (2004). Biodegradation of polycyclic aromatic hydrocarbons (PAHs) by *Cladosporium sphaerospermum* isolated from an aged PAH contaminated soil. *FEMS Microbiology Ecology* 51(1), 71-8.
- Rahman M. S. and Islam M. R. (2009). Effects of pH on isotherms modeling for Cu(II) ions adsorption using maple wood sawdust. *Chemical Engineering Journal* 149, 273–80.
- Sun Y., Yang S., Zhao G., Wang Q. and Wang X. (2013). Adsorption of polycyclic aromatic hydrocarbons on graphene oxides and reduced graphene oxides. *Chemistry – An Asian Journal* 8(11), 2755-61.
- Yakout S. M. and Daifullah A. A. M. (2013). Removal of selected polycyclic aromatic hydrocarbons from aqueous solution onto various adsorbent materials. *Desalination and Water Treatment* 51(34-36), 6711-8.